ISSN 1062-8738, Bulletin of the Russian Academy of Sciences: Physics, 2017, Vol. 81, No. 3, pp. 320–322. © Allerton Press, Inc., 2017.
Original Russian Text © S.F. Kiseleva, N.A. Koneva, N.A. Popova, Ed.V. Kozlov, 2017, published in Izvestiya Rossiiskoi Akademii Nauk, Seriya Fizicheskaya, 2017, Vol. 81, No. 3, pp. 349–351.

Tensor of Internal Stresses in Polycrystalline Grains with Complex Bending

S. F. Kiseleva*, N. A. Koneva, N. A. Popova, and Ed. V. Kozlov

Tomsk State University of Architecture and Building, Tomsk, 634003 Russia

**e-mail: kisielieva1946@mail.ru*

Abstract—Processes that occur upon the straining of a polycrystal are studied. Components of the internal stress tensor were determined. Changes in the bending and torsion stresses in the crystal lattice of a strained polycrystal are analyzed. A correlation between changes in the internal stress tensor components and the fraction of material with complex bending is established.

DOI: 10.3103/S1062873817030170

INTRODUCTION

Most alloys are polycrystals. When polycrystals are strained, their crystal lattice is distorted [1, 2], and internal stress fields appear [2–5]. Stressed areas in electron microscopic photos of the structures of strained polycrystals are usually seen to have bending extinction contours that reflect the nature of strain in local areas of the sample and can be identified by the mutual orientation of the extinction contours and effective vector reflection $\vec{g}$ [6]. There are three types of crystal lattice strain: bending, torsion, and combined. Mixed strains are more frequently observed, so we must consider both stress tensor components (i.e., crystal lattice bending and torsion) when determining internal stresses. Internal stresses can be reconstructed from the parameters of bending extinction contours [6].

The aim of this work was to study the changes in internal stress tensor components (crystal lattice bending and torsion components) upon strain versus different types of bending in a material.

DETERMINING INTERNAL STRESS TENSOR COMPONENTS

The internal stresses that characterize strain form second-rank tensors [7]. For cubic crystals, these tensors have only two independent components: bending stress σ_{11} and torsion stress σ_{12} of the crystal lattice. In local areas of a sample, strains can be both plastic and elastoplastic; i.e., plastic and elastic internal stress components exist simultaneously.

Using the method proposed in [8] by the authors of this work for determining the stress tensor components from the parameters of bending extinction contours observed in electron microscopic photos, we found the internal stress tensor components to be

$$\sigma_{11,\mathrm{pl}} = \mu\sqrt{\vec{b}\chi_{11,\mathrm{pl}}}, \quad \sigma_{12,\mathrm{pl}} = \mu\sqrt{\vec{b}\chi_{12,\mathrm{pl}}}, \tag{1}$$

$$\sigma_{11,\mathrm{el}} = \mu t\chi_{11,\mathrm{el}}, \quad \sigma_{12,\mathrm{el}} = \mu t\chi_{12,\mathrm{el}}, \tag{2}$$

where μ is the elasticity modulus; t is the foil thickness; $\vec{b}$ is the Burgers vector; and $\chi_{11,\mathrm{pl}}$, $\chi_{12,\mathrm{pl}}$, $\chi_{11,\mathrm{el}}$, and $\chi_{12,\mathrm{el}}$ are the bending-torsion tensor components

$$\chi_{11,\mathrm{pl}} = \frac{\Delta\varphi}{\Delta L_{x,\mathrm{pl}}}, \quad \chi_{12,\mathrm{pl}} = \frac{\Delta\varphi}{\Delta L_{y,\mathrm{pl}}}, \tag{3}$$

$$\chi_{11,\mathrm{el}} = \frac{\Delta\varphi}{\Delta L_{x,\mathrm{el}}}, \quad \chi_{12,\mathrm{el}} = \frac{\Delta\varphi}{\Delta L_{y,\mathrm{el}}}. \tag{4}$$

Here, $\Delta\varphi$ is the angle of misorientation on length ΔL, and $\Delta L_{11,\mathrm{pl}}$, $\Delta L_{12,\mathrm{pl}}$, $\Delta L_{11,\mathrm{el}}$, and $\Delta L_{12,\mathrm{el}}$ are the extinction contour width projections corresponding to the plastic and elastic components of internal stresses.

RESULTS AND DISCUSSION

The investigated material was 1.1C–13Mn–Fe polycrystalline austenite steel with a grain size of 34 μm. The steel was strained by tension to destruction ($\varepsilon = 36\%$) at room temperature at a rate of $3.4 \times 10^{-4}\ \mathrm{s}^{-1}$ on an Instron machine. Foils prepared from the strained samples were studied on an EM-125K electron microscope at an accelerating voltage of 125 kV. The electron microscope photos of the steel's structure at different levels of strain are shown in Fig. 1. Dislocations that form either chaotic or network structures, single microtwins, packages of microtwins, or bending extinction contours are observed in the photo. In this work, we determined the volumetric fraction of material occupied by microtwins (δ), and

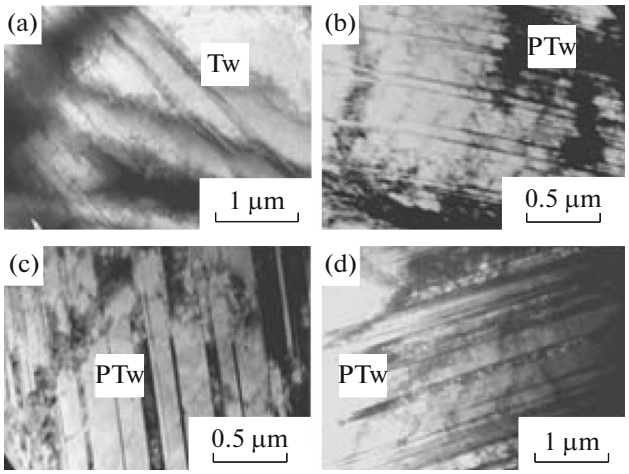

Fig. 1. Electron microscopic photos of the structure of 1.1C–13Mn–Fe strained austenite steel at yield stresses σ of (a) 0.49, (b) 0.69, (c) 1.00, and (d) 1.15 GPa. Tw denotes single microtwins; PTw, packages of microtwins.

the dependence of δ on the yield stress σ was plotted (Fig. 2). The dependences of the number of twinning systems (curve *1*), the average internal stresses (curve *2*), and the fraction of material occupied by microtwins (curve *3*) on the yield stress in the range of 0.49–1.15 GPa are shown in Fig. 2a. The dependences of the bending stress (curve *4*) and torsion stress (curve *5*) of the crystal lattice on the yield stress are plotted in Fig. 2b.

From Fig. 2a, we can see that only one microtwinning system is observed at a yield stress of 0.49 GPa (ε = 5%), while microtwinning occurs *en masse* at σ > 0.49 GPa (ε > 5%). The number of microtwinning systems grows along with the level of strain, from one system at σ > 0.49 GPa (ε = 5%) to two systems at σ = 0.60 and σ = 0.69 GPa (ε = 10 and 14%), three systems at σ = 0.84 GPa (ε > 21%), and even four systems starting at σ > 1.00 GPa (ε > 29%). The fraction of material engaged in microtwinning also grows appreciably in this case. The fraction of twinned material is 0.45 and 0.49 at yield stresses σ = 0.60 and 0.69 GPa (ε = 10 and 14%) and grows to 0.7–0.80 when σ > 0.93 GPa (ε > 25%). The number of microtwinning systems (*N*) and the volumetric fraction of twinned material thus grow along with yield stress. This affects the change in the stress tensor components and the average internal stresses in the material.

The behavior of the bending and torsion stresses (σ_{11}, σ_{12}) of the crystal lattice was studied in yield stress range σ = 0.49–1.15 GPa. From Fig. 2b, we can see that the stress tensor components (σ_{11}, σ_{12}) behave differently as the yield stress grows. Bending stress σ_{11} generally rises to a yield stress of 1.05 GPa and then falls slowly. Torsion stress σ_{12} of the crystal lattice grows only to a yield stress of 0.75 GPa at a higher rate than for σ_{11}. While the yield stress subsequently grows

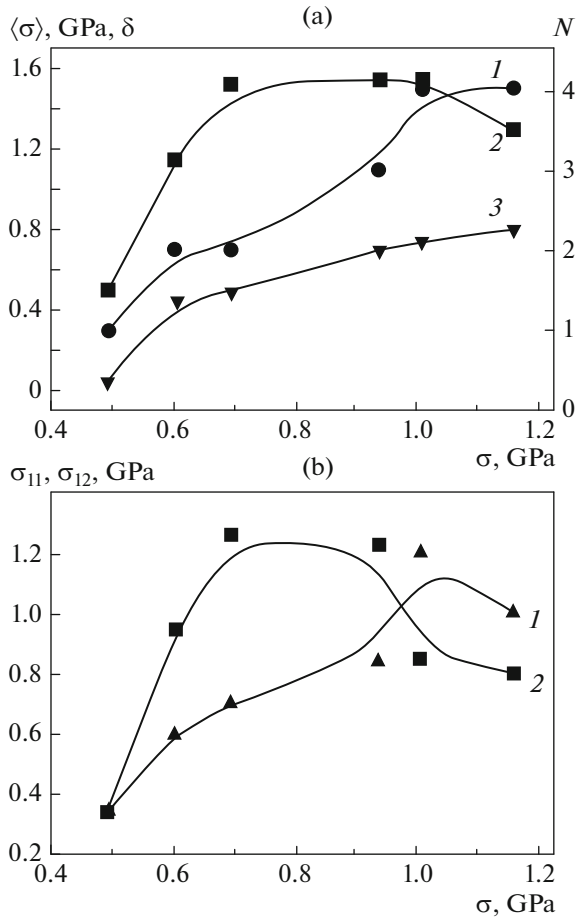

Fig. 2. (a) (*1*) Number of twinning systems, (*2*) average internal stresses, and (3) fraction of material occupied by microtwins; (b) (*4*) bending stress, and (*5*) torsion stress of the crystal lattice of our strained material versus yield stress in the range of 0.49–1.15 GPa.

to σ ≈ 0.84 GPa, torsion stress σ_{12} of the crystal lattice remains virtually the same and then falls to σ = 1.15 GPa. Average internal stresses ⟨σ⟩ in this case first grow (to σ = 0.69 GPa, ε = 14%), and their growth starts to slow at σ = 0.69–0.97 GPa (ε = 14–28%). Internal stresses fall again at σ = 0.97–1.15 GPa (ε = 28–36%). Our results versus the number of microtwinning systems *N*, volumetric twinned material fraction δ, and internal stresses ⟨σ⟩ upon varying yield stress from 0.49 to 1.15 GPa (level of strain ε = 5–36%) are presented in the table.

From the table we can see that while *N* and δ grow along with yield stress, the stress tensor components (bending stress σ_{11} and torsion stress σ_{12} of the crystal lattice) first increase and then decrease. Tensor component σ_{11} is greater than σ_{12} up to σ = 0.93–0.97 GPa; otherwise, the contribution to internal stresses from σ_{11} predominates when σ > 0.97 GPa. The contribution to internal stresses from σ_{12} is then reduced. In [9], it was established that torsion stress σ_{12} of a crystal

Changes in internal stresses and stress tensor components as yield stress grows

Yield stress σ, GPa (level of strain ε, %)	Internal stress ⟨σ⟩, GPa	Bending stress σ_{11}, GPa	Torsion stress σ_{12}, GPa	Volumetric twinned material fraction	Number of material areas with complex bending
0.49–0.69 (5–14)	Grows 0.50–1.51	Grows 0.34–0.71	Grows 0.34–1.26	Increases 0.04–0.49	Increases
0.69–0.93 (14–25)	Grows slowly 1.50–1.54	Grows 0.71–0.84	Changes slightly 1.26–1.23	Increases 0.49–0.70	Changes slightly
0.93–0.97 (25–28)	Nearly constant 1.54–1.55	Grows 0.84–1.20	Decreases 1.23–0.85	Increases 0.70–0.73	Decreases
0.97–1.15 (28–36)	Decreases 1.55–1.15	Decreases slowly 1.20–1.00	Decreases slowly 0.85–0.80	Increases 0.73–0.80	Decreases

lattice in areas of a material with complex bending is always greater than in areas with simple bending at the same level of strain. The growth of σ_{12} is typical for areas of a material with complex bending; i.e., if the fraction of the material with complex bending increases, the stress tensor component representing the torsion stress of the crystal lattice also grows. It follows that the fraction of material with complex bending grows as the yield stress rises from 0.49 to 0.69 GPa. In addition, the number of such areas grows slightly when $\sigma = 0.69–0.97$ GPa and falls when $\sigma >$ 0.97 GPa.

CONCLUSIONS

Stress tensor component σ_{12} in 1.1C–13Mn–Fe austenite steel first grows along with strain and then falls. Microtwinning occurs in the steel under strain. Tensor component σ_{12} declines when the third microtwinning system occupies a major fraction of the material, and tensor component σ_{11} also falls when the fourth microtwinning system appears, thus promoting the relaxation of stresses. In addition, microcracks appear prior to destruction of the steel. This also favors the relaxation of stresses. The internal stress tensor components (the bending and torsion stresses of the crystal lattice) decline. Prior to destruction, the fraction of material with complex bending becomes lower than for the material with simple bending.

ACKNOWLEDGMENTS

This work was supported by the Russian Foundation for Basic Research, project no. 16-48-700198.

REFERENCES

1. Panin, V.E., Panin, A.V., Elsukova, T.F., and Popkova, Yu.F., *Phys. Mesomech.*, 2015, vol. 18, no. 2, p. 89.
2. Koneva, N.A., Kozlov, E.V., Trishkina, L.I., and Lychagin, D.V., in *Novye metody v fizike i mekhanike deformiruemogo tverdogo tela. Chast' 1* (New Methods in Physics and Mechanics of a Deformed Solid Body. Part 1), Panin, V.E., Ed., Tomsk: Tomsk. Gos. Univ., 1990, p. 83.
3. Konstantinova, T.E., *Mezostruktura deformirovannykh splavov* (Mesostructure of Deformed Alloys), Donetsk: Donetsk. Fiz.-Tekh. Inst., 1997.
4. Koneva, N.A. and Kozlov, E.V., in *Strukturno-fazovye sostoyaniya i svoistva metallicheskikh sistem* (Structure and Phase States and Properties of Metallic Systems), Potekaev, A.I., Ed., Tomsk: Izd. Nauchno-Tekh. Lit., 2004, p. 83.
5. Tyumentsev, A.N., Ditenberg, I.A., Korotaev, A.D., and Denisov, K.I., *Phys. Mesomech.*, 2013, vol. 16, no. 4, p. 319.
6. Kozlov, E.V., Lychagin, D.V., Popova, N.A., et al., in *Fizika prochnosti geterogennykh materialov* (Physics of Strength of Heterogeneous Materials), Romanov, A.E., Ed., Leningrad: Fiz.-Tekh. Inst., 1988, p. 3.
7. Smirnov, A.A., *Molekulyarno-kineticheskaya teoriya metallov* (Molecular-Kinetic Theory of Metals), Moscow: Nauka, 1966.
8. Kiseleva, S.F., Popova, N.A., Koneva, N.A., and Kozlov, E.V., *Fundam. Probl. Sovrem. Materialoved.*, 2012, vol. 9, no. 1, p. 7.
9. Gibert, I.A., Kiseleva, S.F., Popova, N.A., and Koneva, N.A., *Sb. nauchn. trudov XIII Mezhdunar. konf. studentov i molodykh uchenykh "Perspektivy razvitiya fundamental'nykh nauk"* (Proc. XIII Int. Conf. of Students and Young Scientists "Prospects for Development of Fundamental Sciences"), Tomsk, 2016, p. 94.

Translated by E. Glushachenkova